Validation of the multinucleon transfer method for the determination of the fission barrier height

K. R. Kean,[1,2] K. Nishio,[2] K. Hirose,[2] M. J. Vermeulen,[2] H. Makii,[2] R. Orlandi,[2] K. Tsukada,[2]
A. N. Andreyev,[2,3] I. Tsekhanovich,[4] and S. Chiba[1]

[1]*Laboratory for Advanced Nuclear Energy, Institute of Innovative Research, and Department of Trans-Disciplinary Science and Engineering, School of Environment and Society, Tokyo Institute of Technology, 2-12-1-N1-19, Ookayama, Meguro-ku, Tokyo 152-8550, Japan*

[2]*Advanced Science Research Center, Japan Atomic Energy Agency (JAEA), Tokai, Ibaraki 319-1195, Japan*

[3]*Department of Physics, University of York, York YO10 5DD, United Kingdom*

[4]*University of Bordeaux, 351 Cours de la Libration, 33405 Talence Cedex, France*

(Received 23 April 2019; published 23 July 2019)

The validity of the multinucleon transfer (MNT) approach for deduction of fission barrier heights was investigated in an experiment carried out at the JAEA tandem accelerator facility. By using the $^{18}O + ^{237}Np$ reaction, fission barrier heights were inferred from fission probabilities of the nuclei ^{239}Np and $^{239,240}Pu$ produced in the $2n$ and $pn/p2n$ transfer channels, respectively. The deduced values of fission barriers agree well with the literature data, thus demonstrating the potential of the MNT reactions for obtaining fission-barrier data for nuclei not accessible for fission studies via neutron- or light charged particle-induced reactions.

DOI: 10.1103/PhysRevC.100.014611

I. INTRODUCTION

Nuclear fission was discovered 80 years ago and remains one of the most challenging subjects in nuclear physics, both experimentally [1,2] and theoretically [2,3]. Nevertheless, nuclear fission is routinely used in power reactors, which generate about 11% of electricity worldwide. The nuclear fission is also important in the astrophysical r-process (fission recycling) [4].

The fission barrier height, introduced by Bohr and Wheeler [5], is one of the most fundamental quantities to describe fission. In the classical liquid-drop picture, the fission barrier is created by a balance between the attractive surface energy and the repulsive Coulomb force of the initial nucleus, and of the nascent fission fragments, which evolve as a function of deformation in a rather simple (parabolic) way. The single-humped fission barrier, which arises in the macroscopic liquid drop approach, is dramatically modified by introducing shell correction energies [6]. These microscopic corrections deform the smooth parabolic barrier form, producing a series of local maxima and minima known as double- or triple-humped fission-barrier profile, see, e.g., Fig. 2 of Ref. [7].

Up until now, information on the fission barrier profile in actinide nuclei has been derived using neutron-induced fission and nucleon-transfer reactions with light projectiles, such as (d, p) [8–10], (t, p) [9,11], and $(^3He, d)$ [12] reactions. In these methods, the fission probability is usually measured as a function of excitation energy of the fissioning nucleus. The height of the fission barrier is then equal to the excitation energy of the nucleus, corresponding to the half-maximum of the fission probability curve for the first chance fission [13]. However, such methods require the use of stable or long-lived target nuclei, which limits the range of accessible nuclei along the β-stability line, and thus the number of the isotopes which can serve as targets for such kind of studies. This explains the relative scarcity of the available experimental data on the fission barrier profile: to our knowledge, there are fission barrier data available on just 33 nuclei in the best-studied actinide region [14,15], out of a few hundred known between uranium and californium.

Recently, we have demonstrated that reliable fission data, e.g., fission fragment mass and kinetic-energy distributions, can be assessed via multinucleon transfer (MNT) reactions of an ^{18}O beam interacting with actinide targets, such as ^{232}Th, ^{238}U, etc. [16,17]. Due to a large number of MNT channels accessible in reactions with an ^{18}O beam, low-energy fission data for about 12 nuclides can be simultaneously taken in a single experiment. For instance, the study [17] reports on the fission fragment mass distributions (FFMDs) for 12 isotopes of uranium, neptunium, and plutonium measured in the $^{18}O + ^{238}U$ reaction.

The present article deals with the extension of the MNT method for determining the fission-barrier height. For a given excitation energy, due to the use of a relatively heavy projectile (^{18}O), the excited states populated in the fissioning nucleus can be different in terms of spin and parity compared to those created in traditional neutron-induced or one- or two-nucleon transfer reactions with light projectiles, such as ^3He. This may result in a different fission probability, and thus may affect the fission-barrier height. Therefore, it becomes important to benchmark the MNT technique by comparing the data on fission probabilities and barriers with available literature data.

II. EXPERIMENT AND DATA ANALYSIS

A. Experiment

The fission of nuclei produced in the MNT channels of the $^{18}O + ^{237}Np$ reaction was studied by using the ^{18}O beam with an energy of 162 MeV and an intensity of 0.5 pnA,

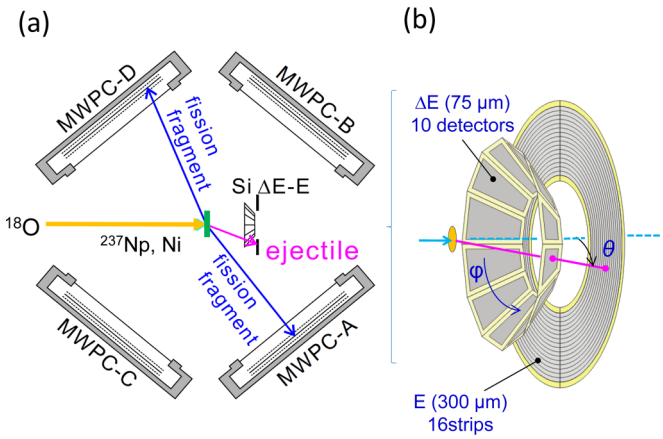

FIG. 1. Schematic representation of the experimental setup. (a) shows the arrangement of the four MWPCs surrounding the ^{237}Np(+Ni) target used to detect the fission fragments, and the ΔE-E telescope used to identify the ejectiles. (b) gives the expanded view of the ΔE-E detector.

supplied by the JAEA tandem accelerator in Tokai, Japan. The target was made by electrodeposition of the ^{237}Np material with a thickness of 76.3 μg cm^{-2} on a natural nickel backing (300 μg cm^{-2}). To quantify the contribution from the backing (i.e., interaction of ^{18}O with $^{\text{nat}}$Ni) to the measured data, a dummy $^{\text{nat}}$Ni target (300 μg cm^{-2} thick) was used with identical beam and geometry conditions.

The detection system was composed of four multiwire proportional counters [MWPCs, cf. Fig. 1(a)] and of a segmented silicon ΔE-E telescope placing at forward angles [cf. Fig. 1(b)]; a more detailed description of the experimental setup can be found in [16]. The MWPC detectors serve for the detection of fission events, whereas the ΔE-E telescope measures specific energy loss and total kinetic energy of the ejectiles. A combination of the ΔE and E signals allows for the ejectile to be unambiguously identified (cf. Fig. 2), as well as for the excitation energy, E^*, of the exit channel to be determined, as explained in [16]. It was shown that this setup can measure E^* to a precision of 0.9 MeV (FWHM, [16]), with the major source coming from the uncertainty on the ejectile kinetic-energy measurement. The mass and proton numbers of the fissioning nucleus produced in a specific MNT channel are obtained from the identified ejectile and the reaction mass/charge balance, by assuming a binary reaction process which is appropriate at the low-excitation energies considered in this work.

B. Data analysis

Examples of particle identification plots (PID) with the ΔE-E detector are given in Fig. 2. Panels (a) and (b) show the registered ejectile data for the ^{237}Np(+$^{\text{nat}}$Ni) and dummy

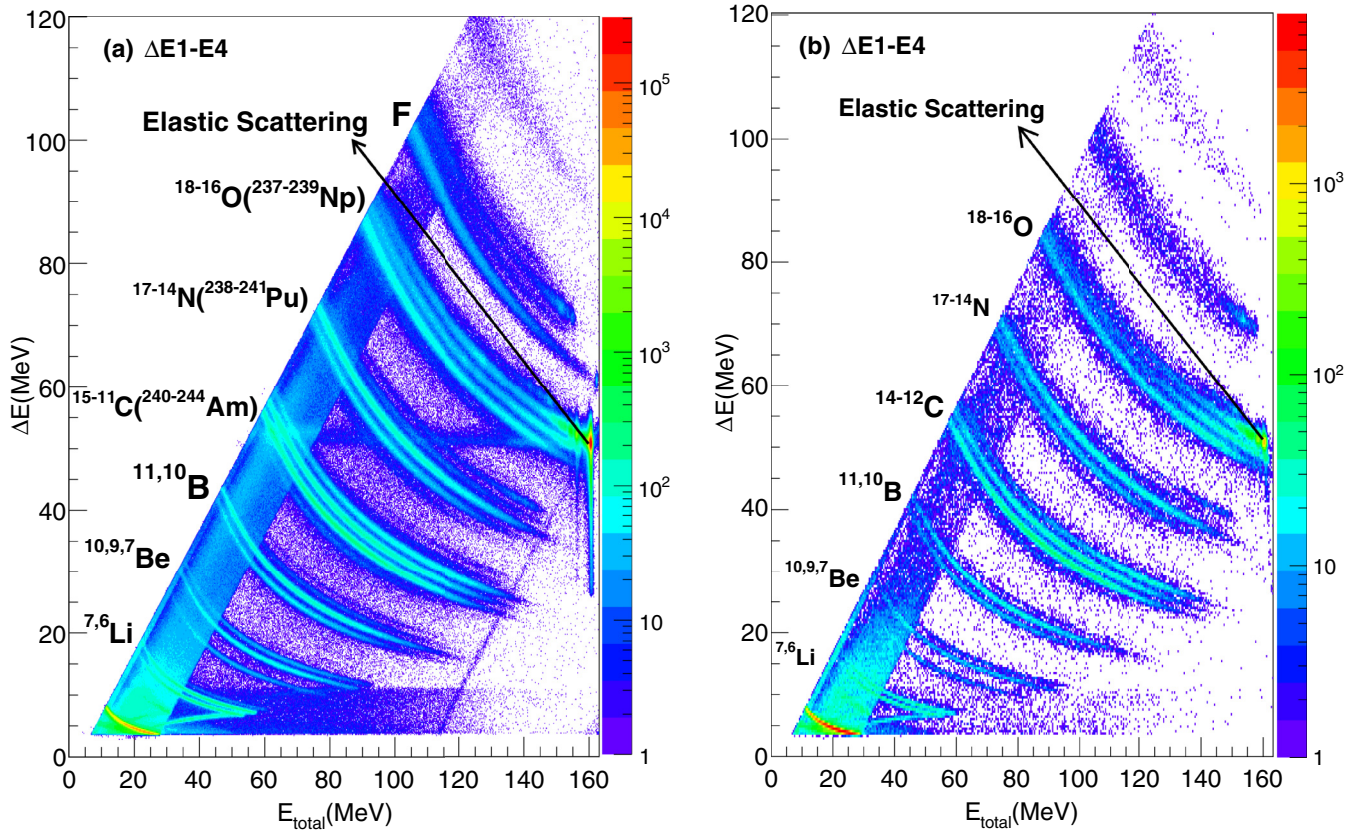

FIG. 2. Energy loss versus total energy obtained from the $\Delta E - E$ telescope. Panel (a) and (b) are obtained using ^{18}O + ^{237}Np(+$^{\text{nat}}$Ni) and ^{18}O + $^{\text{nat}}$Ni, respectively, with a beam dose of 2.0×10^6 and 8.2×10^5, respectively.

^{nat}Ni targets, respectively. The different (A, Z) lines associated with specific ejectiles are well separated, making it possible to identify specific reaction channels clearly. On each plot, we applied banana-like gates, using a functional to select the charge and mass of the ejectile in the ΔE-E telescope by using the method outlined in [18]. For the interpretation of the experimental data hereafter, we assume that all the excitation energy in the exit channel is given to the compound nucleus. This assumption is similar to our analysis in [17].

For every E^* value, the fission probability P_f can be extracted from the recorded data with the help of the following expression:

$$P_f(E^*) = \frac{N_{ej}^{coin}(E^*)}{N_{ej}^{sing}(E^*)\varepsilon(E^*)}. \quad (1)$$

Here, N_{ej}^{coin} is the number of the selected ejectiles in coincidence with both fission fragments, N_{ej}^{sing} is the total number of the selected ejectiles (=singles), and ε is the fission detection efficiency.

Figure 3 demonstrates details of the analysis for the specific transfer channel ^{237}Np(^{18}O, ^{15}N)^{240}Pu. A 0.8 MeV bin size was used for the excitation energy in Fig. 3 which is a compromise between the number of events (statistics) in each bin and the uncertainty on the excitation energy. Figure 3(a) shows a singles energy spectrum of the ^{15}N ejectiles recorded with the ^{237}Np(+^{nat}Ni) and dummy targets (blue rectangles and yellow triangles, respectively), which are taken from the corresponding data in Figs. 2(a) and 2(b). The difference between the two curves (red circles) is the net ejectile spectrum related to the ^{237}Np target. This subtraction was done after normalization on the beam dose evaluated from the elastically scattered peak of ^{18}O. Figure 3(b) gives the ^{15}N data from Fig. 3(a), coincident with fission events in the MWPCs (blue rectangles). This part of the data can be affected by random coincidences (black stars) with events from the different origin, included in the ejectile-fragment coincidence gate (2 μs). It should be noted that random coincidences are very significant for the $^{16-18}$O ejectiles, particularly at the excitation energies of 0–5 MeV. This is due to the influence of events from scattering (see the horizontal ^{18}O beam tail in Fig. 2), which are not entirely suppressed by the fragment-fragment-ejectile condition used in the data analysis. However, it can be seen in Fig. 3(b) that the impact of random coincidences on the remaining ejectile data is negligible. The red circles in Fig. 3(b) show the result after subtracting the random coincidence events from the coincidence spectrum.

By using Eq. (1) and the background subtracted data from Fig. 3(a) and (b), the P_f(^{240}Pu) distribution was obtained, as shown in Fig. 3(c).

The efficiency, mainly determined by the solid angle covering by the MWPCs, is 7.5% after accounting for a 25% of shadowing the two forward-placed MWPCs by the ΔE-E telescope. Owing to the fact that the fission setup was able to detect both fission fragments, the efficiency correction was determined for each transfer channel according to the formula

$$\varepsilon = 7.5\% \times \frac{N_1}{N_2}, \quad (2)$$

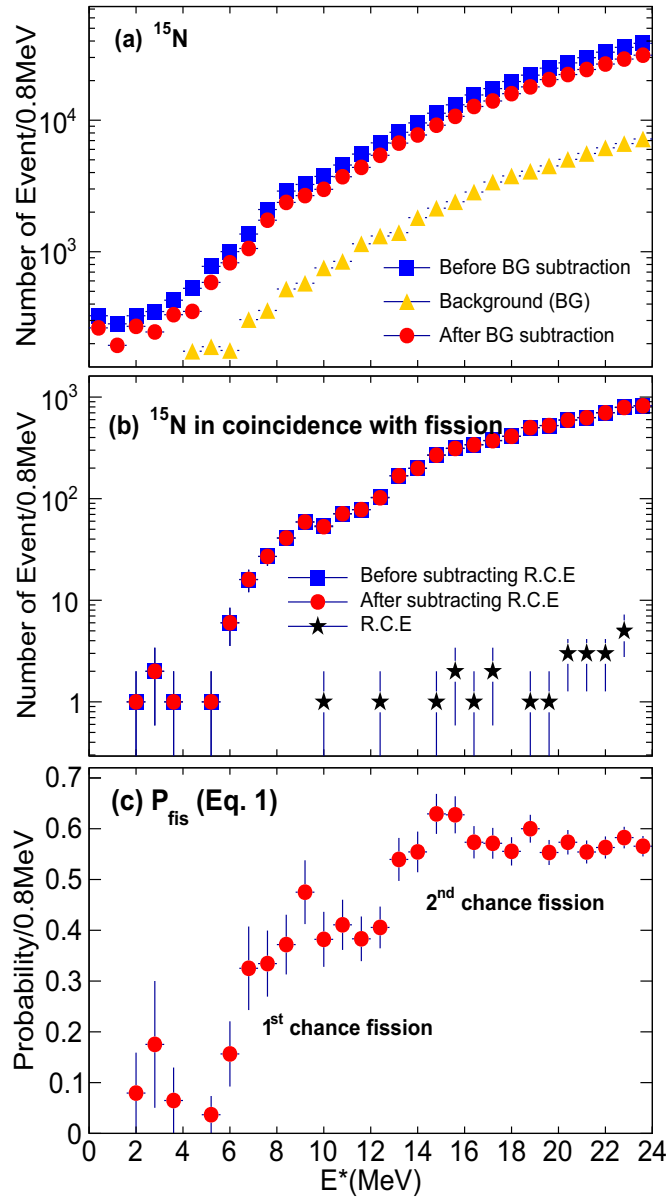

FIG. 3. Data for the ^{237}Np(^{18}O, ^{15}N)^{240}Pu reaction. (a) Singles spectra for ^{15}N as measured in the $\Delta E - E$ telescope, see main text for details. (b) Spectra for ^{15}N events from the $\Delta E - E$ telescope in coincidence with fission fragments detected by the MWPCs. R.C.E stands for random coincidence events. (c) Deduced fission-probability (P_f) spectrum. The increase in P_f at 6.50 MeV and at ~14 MeV is due to the 1st and 2nd fission chances of ^{240}Pu, respectively.

where N_1 and N_2 stand for the number of ejectiles coincident with both fission fragments (triple coincidence) and with fragments detected by backward MWPC (double coincidence), respectively. The dependence of ε on the transfer channel was found to be rather small: $\varepsilon = 4.28(21)\%$, $4.82(24)\%$, $4.65(23)\%$ for ^{237}Np(^{18}O, ^{16}O)^{239}Np, ^{237}Np(^{18}O, ^{16}N)^{239}Pu, and ^{237}Np(^{18}O, ^{15}N)^{240}Pu reactions, respectively. Similarly, only a weak dependence of ε on E^*, not exceeding 5%, was

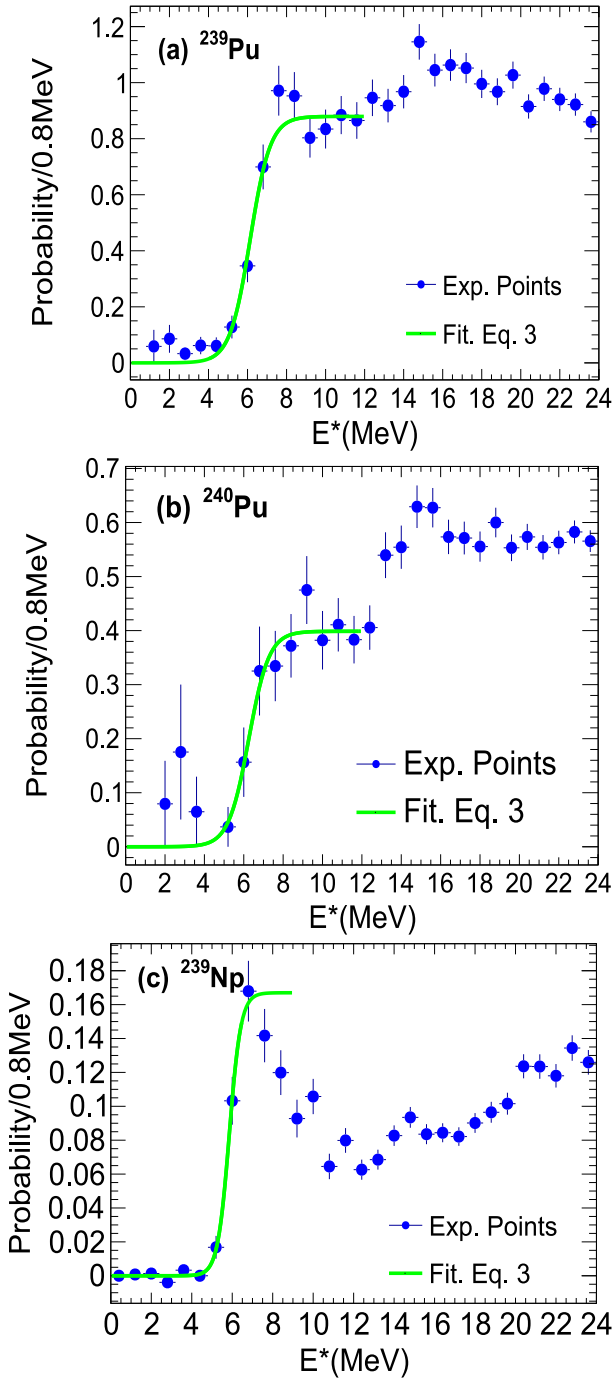

FIG. 4. Fission probability as a function of excitation energy for ^{239}Pu (a), ^{240}Pu (b) and ^{239}Np (c). Green solid line on each plot shows the fit function from Eq. (3) applied to the sub-barrier and first-chance fission parts of the data only.

deduced. The insensitivity of the efficiency to the excitation energy was also found in the comprehensive study [19].

Figure 4 presents fission probabilities (blue filled symbols) for the np, $2np$, and $2n$ transfer channels for the ^{237}Np(^{18}O, ^{16}N)^{239}Pu, ^{237}Np(^{18}O, ^{15}N)^{240}Pu, and ^{18}O, ^{16}O)^{239}Np reactions, respectively. The three isotopes are of great interest for the nuclear power cycle which explains the availability of a wealth of experimental data on their fission probabilities and barriers, thus making them suitable candidates for benchmarking the MNT method.

The uncertainties on the fission probabilities shown in Fig. 4 are calculated according to the prescription given in [19], but without taking into account the covariance terms: even though it may lead to an overestimation of the uncertainty by ≈30% [19].

C. Fitting method

The selected bin of 0.8 MeV for the plots in Fig. 4 results in just a few data points in the rising—and most important—part of the fission probability (P_f) curves. This rather poor energy resolution excludes observation of any resonance (class-II) sub-barrier structures, which are sensitive to both the inner and outer barrier heights [15]. On the other hand, it is well known [20] that the use of a single-humped, Hill-Wheeler-type approximation allows a consistent derivation of the height of the barrier to be made, corresponding to the higher one as determined by the models involving the two-humped fission barrier description.

Consequently, in the present work, the fission barrier heights were deduced from the P_f curves from Fig. 4, fitted with the Hill-Wheeler's expression for the barrier penetration [21]:

$$P_f(E^*) = \frac{P_{\max}}{1 + \exp\left(\frac{2\pi(B_f - E^*)}{\hbar\omega}\right)}, \tag{3}$$

where the three fitting parameters $P_{\max}$, B_f, and $\hbar\omega$ represent the maximum fission probability reached by the first chance fission, the fission barrier height, and its curvature, respectively. The fitting was performed using CERN ROOT code using a χ-square method, over the range of the sub-barrier and first-chance fission. The fitted curves are shown in Fig. 4 in green, whereas the deduced B_f are compared to literature values in Table I. The obtained curvatures are in the range of 1–5 MeV, which in general is largely different from 1 MeV known from the literature. However, the fission-barrier curvature cannot be deduced in a correct way with this approach (simply inverted parabola), which replaces the complex (in general, two-humped) barrier structure in actinide nuclei. Therefore, in the following, only P_f and B_f will be considered.

III. RESULTS AND DISCUSSIONS

The fission barrier heights of the three nuclei ^{239}Np and ^{239,240}Pu were determined to be $B_f(^{239}\text{Np}) = 5.86(9)$ MeV, $B_f(^{239}\text{Pu}) = 6.14(12)$ MeV, and $B_f(^{240}\text{Pu}) = 6.25(32)$ MeV. Table I compares the obtained B_f values with the RIPL3 library [14] (evaluation from the neutron-induced cross sections), as well as with known data from several transfer reactions using light projectiles, such as ^{238}Pu(t, p)^{240}Pu [11] and ^{238}U(^{3}He, d)^{239}Np [12]. We note that the cited literature data [11,12,14] provide information on the first (inner) and the second (outer) barrier height (cf. Table I).

It follows from the table that our B_f values agree well with the maxima of the two barrier heights, i.e., with the inner barrier height, for the studied nuclei. In particular, this

TABLE I. Fission barrier heights B_f for ^{239}Np and ^{239,240}Pu isotopes from this work, in comparison to the literature data.

Isotope	Reference	B_f(MeV)(inner, outer)
^{239}Np	This work: (^{237}Np(^{18}O, ^{16}O)^{239}Np)	5.86 ± 0.09
	RIPL3 [14]	—
	^{238}U(^{3}He, d)^{239}Np [12]	5.85 ± 0.30, 5.50 ± 0.30
^{239}Pu	This work: (^{237}Np(^{18}O, ^{16}N)^{239}Pu)	6.14 ± 0.12
	RIPL3 [14]	6.20, 5.70
^{240}Pu	This work: (^{237}Np(^{18}O, ^{15}N)^{240}Pu)	6.25 ± 0.32
	RIPL3 [14]	6.05, 5.15
	^{238}Pu(t, p)^{240}Pu [11]	5.80 ± 0.20, 5.45 ± 0.20

agreement remains within a one-sigma interval with the transfer-reaction results, carried out for actinide nuclei using transfer reactions [10,11]. By using a statistical model including the double-humped fission barrier concept to describe the fission decay, peaks, and curvatures for two barriers were determined for some cases, but only information for one of the barriers is given for all other cases. As for the empirical data from RIPL3 [14], their inner barrier heights are reproduced by our results with high precision: within 1% for ^{239}Pu and 4% for ^{240}Pu.

Fission probabilities from Fig. 4 are of importance, from the point of view of reaction rate calculations for given conditions (reactor or stellar neutron spectra, for instance). In this respect, it is worth noting to say that transfer reactions are the only tool to access the low-energy part of the P_f spectrum (i.e., below the neutron-separation energy S_n) in nuclei with an even number of neutrons (i.e., for which $B_f \leqslant S_n$).

For the maximal values of the P_f of the compound nuclei in Fig. 4, we observe some discrepancies between our results and the literature data obtained using lighter ion beams [11,12,22,23]. In particular, for ^{240}Pu formed in the ^{236}U(^{12}C, ^{8}Be) reaction [23] one obtains $P_{\max} = 0.6$ at $E^* = 8$ MeV, whereas our experiment delivers a somewhat lower value of $P_{\max} = 0.4$, at the same excitation energy. This discrepancy increases for ^{239}Np studied in the ^{239}U(^{3}He, t)^{239}Np reaction [22], where $P_{\max} = 0.7$ at $E^* = 6$ MeV is significantly larger than the present result of $P_{\max} = 0.17$ ($E^* = 7$ MeV). Finally, the ^{238}Pu(d, p)^{239}Pu reaction delivers $P_{\max} = 0.5$ at $E^* = 7$ MeV [12] for ^{239}Pu, in contrast to our value of $P_{\max} = 0.9$.

Concerning the latter case, it is well established [8] that results from a (d, p) reaction should be corrected for the deuteron breakup, which creates protons as ejectiles and leads to an overestimation of the event number in the singles spectrum and, consequently, to an underestimation of the fission probabilities.

Our lower P_f values for ^{239}Np and ^{240}Pu nuclei can be explained by the difference in the geometry between the present and the mentioned experiments (the ejectile detector angle relative to the beam axis), which makes the final results sensitive to the induced angular momentum effect, which alters level densities that affect fission probability sensitively.

The above conjecture is strongly supported by our experimental data. In particular, one observes that the magnitude of the fission probability is sensitive to the angle of the registered ejectile, given by the ring of the ΔE-E telescope, with respect to the beam direction. For example, in the ^{237}Np(^{18}O, ^{16}O)^{239}Np reaction, the $P_{\max}$ value can be changed by a factor of two. The P_f dependence on the ejectile angle was also observed in the ^{238}U(d, p) reaction, though the effect was found to be smaller [8]. The magnitude of the effect is expected to be linked to the projectile mass (^{18}O in the present study and ^{3}He in [8]); this topic makes a subject for dedicated further study.

IV. CONCLUSIONS

The demonstrated agreement of the B_f results obtained in the present study with known fission-barrier data from different neutron (RIPL3) and particle-transfer [(t, p), (^{3}He, d)] reactions allows one to extend the validity of the transfer-reaction technique for the fission-barrier studies to the ^{18}O beam.

In the present work, the fission barrier heights of ^{239}Np, ^{239,240}Pu nuclei were deduced by using MNT-induced fission reactions. A good agreement between the previously known data, originating from neutron-induced and particle-induced reactions, was demonstrated. This fact allows one to confirm the validity of the MNT method.

We find that the MNT-technique with a heavy ion beam, e.g., ^{18}O as in this case, allows for a variety of compound nuclei to be created and simultaneously investigated for fission properties. In particular, the ^{18}O + ^{237}Np MNT reactions producing oxygen, nitrogen, and carbon isotopes as ejectiles can be used for determination of the fission-barrier, as they produce fissioning isotopes at sufficiently low excitation energies. In contrast to this, the compound nuclei of curium, berkelium, and californium corresponding to light ejectiles such as boron, beryllium, and lithium, respectively, are poorly produced at the excitation energies comparable with, or below, the fission-barrier height. This reduced the number of the MNT channels suitable for fission-barrier studies. However, the fission barriers of heavier nuclei can be accessed by using MNT reactions on heavier and more exotic target nuclei, such as ^{244}Pu, ^{243}Am, ^{249}Cm, ^{249}Bk, ^{249}Cf.

In summary, direct-kinematics MNT reactions using ^{18}O as a projectile are a useful tool for a simultaneous determination

of fission-barrier heights for a wide range of nuclei in the actinide region.

ACKNOWLEDGMENTS

The study is made in the framework of the project "Comprehensive study of delayed-neutron yields for an accurate evaluation of kinetics of high burn-up reactors" supported by the Ministry of Education, Culture, Sports, Science and Technology of Japan (MEXT). K.R.K. acknowledges the support from the MEXT scholarship program for Cambodian citizens. The authors thank the tandem accelerator operators who provided the high-quality ^{18}O beam. A.N.A. acknowledges the support by the UK Nuclear Data Network funded by the UK Science and Technology Facilities Council Grant No. ST/N00244X/1.

[1] A. N. Andreyev, K. Nishio, and K. H. Schmidt, Rep. Prog. Phys. **81**, 016301 (2018).
[2] K. H. Schmidt and B. Jurado, Rep. Prog. Phys. **81**, 106301 (2018).
[3] N. Schunck and L. M. Robledo, Rep. Prog. Phys. **79**, 116301 (2016).
[4] M. Eichler *et al.*, Astrophys. J. **808**, 30 (2015).
[5] N. Bohr and J. A. Wheeler, Phys. Rev. **56**, 426 (1939).
[6] V. M. Strutinsky, Nucl. Phys. A **122**, 1 (1968).
[7] A. V. Karpov *et al.*, J. Phys. G: Nucl. Part. Phys. **35**, 035104 (2008).
[8] Q. Ducasse *et al.*, Phys. Rev. C **94**, 024614 (2016).
[9] H. C. Britt and J. D. Cramer, Phys. Rev. C **2**, 1758 (1970).
[10] P. Glässel *et al.*, Nucl. Phys. A **256**, 220 (1976).
[11] B. B. Back *et al.*, Phys. Rev. C **9**, 1924 (1974).
[12] B. B. Back *et al.*, Phys. Rev. C **10**, 1948 (1974).
[13] R. Vandenbosch and J. R. Huizenga, *Nuclear Fission* (Academic Press, New York, 1973).
[14] https://www-nds.iaea.org/RIPL-3/fission/empirical-barriers.dat.
[15] S. Bjørnholm and J. E. Lynn, Rev. Mod. Phys. **52**, 725 (1980).
[16] R. Léguillon *et al.*, Phys. Lett. **761**, 125 (2016).
[17] K. Hirose *et al.*, Phys. Rev. Lett. **119**, 222501 (2017).
[18] L. Tassan-Got, Nucl. Instrum. Methods Phys. Res. B **194**, 503 (2002).
[19] G. Kessedjian *et al.*, Phys. Rev. C **91**, 044607 (2015).
[20] J. D. Cramer and J. R. Nix, Phys. Rev. C **2**, 1048 (1970).
[21] D. L. Hill and J. A. Wheeler, Phys. Rev. **89**, 1102 (1953).
[22] A. Gavron *et al.*, Phys. Rev. C **13**, 2374 (1976).
[23] E. Cheifetz, H. C. Britt, and J. B. Wilhelmy, Phys. Rev. C **24**, 519 (1981).